Cement and Concrete Research 40 (2010) 1226–1236

Contents lists available at ScienceDirect

Cement and Concrete Research

journal homepage: http://ees.elsevier.com/CEMCON/default.asp

Modelling and simulations of the chemo-mechanical behaviour of leached cement-based materials: Interactions between damage and leaching

E. Stora [a,b,*], B. Bary [a], Q.-C. He [b], E. Deville [c], P. Montarnal [c]

[a] Atomic Energy Commission, CEA Saclay DEN/DANS/DPC/SCCME/Laboratoire d'Etude du Comportement des Bétons et des Argiles, 91191 Gif sur Yvette, France
[b] Université Paris-Est, Laboratoire de Modélisation et Simulation Multiéchelle, FRE3160 CNRS, 5 boulevard Descartes, 77454 Marne-la-Vallée Cedex 2, France
[c] CEA Saclay DEN/DANS/DM2S/SFME/MTMS, 91191 Gif sur Yvette, France

ARTICLE INFO

Article history:
Received 26 February 2008
Accepted 8 April 2010

Keywords:
Mechanical properties (C)
Diffusion (C)
Degradation (C)
Micromechanics (C)
Modeling (E)

ABSTRACT

The assessment of the durability of cement-based materials, which could be employed in underground structures for nuclear waste disposal, requires accounting for deterioration factors, such as chemical attacks and damage, and for the interactions between these phenomena. The objective of the present paper consists in investigating the long-term behaviour of cementitious materials by simulating their response to chemical and mechanical solicitations. In a companion paper (Stora et al., submitted to Cem. Concr. Res. 2008), the implementation of a multi-scale homogenization model into an integration platform has allowed for evaluating the evolution of the mineral composition, diffusive and elastic properties inside a concrete material subjected to leaching. To complete this previous work, an orthotropic micromechanical damage model is presently developed and incorporated in this numerical platform to estimate the mechanical and diffusive properties of damaged cement-based materials. Simulations of the chemo-mechanical behaviour of leached cementitious materials are performed with the tool thus obtained and compared with available experiments. The numerical results are insightful about the interactions between damage and chemical deteriorations.

1. Introduction

The service life of cement-based materials, which can serve as engineering barriers for the disposal of long-term nuclear waste, is affected by different deterioration factors, such as chemical attacks and mechanical damage. The present paper is focused on the modelling and simulations of two particular sources of degradation that may interact with each other and have detrimental consequences on concrete underground facilities: (i) dissolution–precipitation reactions caused by ionic migration, governed by the material transport properties, between the interstitial solution and ground water; and (ii) damage due for instance to external mechanical loadings.

Various experimental studies evidence significant negative interactions between these deterioration factors. For example, Tognazzi [1] showed the existence of highly degraded areas around notches representing artificial cracks similar to those originated by mechanical damage. Hence, the nucleation and growth of cracks in the concrete may accelerate the transport phenomena and enhance the chemical degradation process, which in turn creates an additional porosity that affects its overall mechanical behaviour. In addition, numerous investigations dedicated to the influence of calcium leaching on the residual mechanical behaviour of cement-based materials (e.g. [2–7]) have concluded on the significant reduction of their elastic moduli and residual strength. They generally consist in performing mechanical tests such as uniaxial compression or traction tests (e.g. [2,4–7]) or 3 point flexion tests (e.g. [4]), on samples previously submitted to an accelerated leaching. Other experiments, designated as "life-time", have been performed by Le Bellégo [4] and Schneider and Chen [8,9], in which a mortar or concrete beam is subjected both to a mechanical loading and a chemical attack by an aggressive solution of ammonium nitrate. These life-time experiments show in a remarkable way the significance of the detrimental interactions between chemical deterioration and damage, since they may lead to its complete rupture after only a few months [8].

The complexity of the chemo-mechanical couplings involved in the experiments mentioned just above necessitates the use of an advanced numerical tool. The French Atomic Energy Commission (CEA) has developed, in collaboration with the French National Agency for Nuclear Waste Management (ANDRA) and Electricité de France (EDF), a numerical integration platform ALLIANCES capable of simulating problems that couple chemistry, transport and mechanics [10,11]. This platform allows for a more thorough modelling of chemo-mechanical degradations compared to existing approaches (e.g. [12–15]) by gathering within the same simulation environment a code solving chemical equilibrium and a finite volume or element software dealing with transport and mechanical problems. In a companion paper [16], a multi-scale homogenization approach has already been incorporated into this platform for predicting how the mineral composition of a

* Corresponding author. Université Paris-Est, Laboratoire de Modélisation et Simulation Multiéchelle, FRE3160 CNRS, 5 boulevard Descartes, 77454 Marne-la-Vallée Cedex 2, France.
E-mail address: stora@univ-mlv.fr (E. Stora).

0008-8846/$ – see front matter © 2010 Elsevier Ltd. All rights reserved.
doi:10.1016/j.cemconres.2010.04.002

concrete material and its linear elastic and diffusive properties are affected during a leaching process. In order to accurately simulate the chemo-mechanical behaviour of decalcified cementitious materials, it is also necessary to develop and implement into this platform a model capable of estimating the effects of damage on the material diffusive and mechanical properties.

Damage being a complex non-linear dissipative phenomenon, its influence on the mechanical and diffusive properties of cement-based materials is generally evaluated in phenomenological manners among the chemo-mechanical approaches proposed in literature (e.g. [5,7,12–15,17]). With the help of simplifying hypotheses detailed later, the present paper aims at proposing a different method by incorporating an orthotropic micromechanical damage model into the ALLIANCES platform. This micromechanical approach consists basically in proposing a simple representation of cracks at a microscopic level and in computing analytically their impact on the diffusive and mechanical properties of cementitious materials through the utilization of crack density parameters [18] and of an explicit homogenization scheme [19]. In the establishment of the model, the number of material parameters to be identified has been required be as small as possible while capturing all the first-order effects. Moreover, this study takes place in the context of nuclear waste storage where radionuclide migration and radioprotection is of paramount importance. As transfer properties controlling the movement of aggressive species are considerably more impacted in the case of tension-induced microcracking than in the case of a compression-induced one due to a much larger crack opening, we only consider in the following tension-induced damage for simplicity. Then, unilateral effects due to the opening or closure of cracks, frictional effects and plasticity are neglected in the proposed model. But future improvements are in progress to avoid these strong assumptions and extend its domains of validity and application.

In the companion paper [16], the leaching process and induced stiffness reduction of a cement paste have been simulated with ALLIANCES. The additional integration of the micromechanical damage model described in this paper inside this numerical software further allows for estimating the non-linear mechanical behaviour of leached cement-based materials as well as the impact of damage on their chemical deterioration. Diverse simulations of the chemo-mechanical behaviour of leached cementitious materials are then performed and confronted with available experimental data [4] to test the predictive capability of the proposed tool in the case of tension-induced damage.

The present paper is organized as follows. In Section 2, an orthotropic damage model based on micromechanics and on a strain-based evolution law is developed and incorporated into a FE code. In Section 3, simulations of simple decalcified structures loaded in flexion are performed and confrontation of the numerical results with available experimental data [4] is carried out. In the ensuing Section, a method is proposed to account for the retroactive effects of damage on the material diffusivity. Finally, Section 5 is devoted to the simulations of life-time tests so as to complete this study about the interactions between damage and chemical deteriorations.

2. Modelling of damage of cementitious materials

Concrete damage is a complex non-linear dissipative phenomenon, which has been the subject of extensive researches (e.g. [20]). Damage in cement-based materials is generally qualified as quasi-brittle and is caused by the nucleation, growth and coalescence of microcracks. These cracks grow preferentially in certain directions depending on the loads applied thus inducing an anisotropy of the damaged material. Many models, which are more or less phenomenological, have been proposed for treating damage in concrete, one of the most popular approaches being the Mazars model [21,22]. Its success seems mainly due to its simplicity of use in a FE code and to its capacity of accounting in a simple and relatively efficient manner for the differences of behaviour of concrete in tension and in compression. It has been extended to fatigue [23] and recently to anisotropic damage [24]. Aiming at proposing a damage model that can be incorporated into a FE code, the present work adopts a hybrid approach using homogenization techniques to determine the number and nature of damage variables and the free energy for a given damage state but also revisits the main ideas underlying the models of Mazars [21,22] and Desmorat et al. [24]. The application of micromechanics for modelling damage is a promising way to relate the damaged material behaviour to its microstructure. However, relatively few micromechanically-based models have been incorporated in FE codes (e.g. [25,26]), because they are usually more difficult to handle than phenomenological models especially in anisotropic cases.

The ensuing simplifying assumptions are adopted. The undamaged material is considered to be isotropic. The assumptions of small strains and of isothermal conditions are adopted. As already mentioned in the introduction, damage in cement-based materials being quasi-brittle, plasticity may be neglected for simplicity at least in tension, and only tension-induced damage is presently considered, so that the unilateral effects due to the opening or closure of microcracks and the frictional effects are neglected. Further developments and improvements of the model will then consist in taking into account compression-induced damage and residual strains. Note that long-term phenomena like creep may also be of importance in the context of nuclear waste disposal since the service life of storage structures is expected to be of several thousands of years.

As noticed by He and Curnier [27], a damage model within the framework of continuum damage mechanics (e.g. [28]) is generally composed of three parts. First, the damage variables are chosen to characterize as accurately as possible the defects (cracks, voids) of the concerned material. Second, the material behaviour is formulated for a given damage state. For this purpose, homogenization techniques are employed to remedy the lack of uniformity in formulating the free energy function. The evolution laws of the damage variables for a loading history are then established in Section 2.3.

2.1. Definition of state variables

The state variables are defined as the group of variables which current values characterize the physical state of a system at equilibrium. Only mechanical state variables are presently considered. The state variables are constituted of the macroscopic strain $\bar{\varepsilon}$ associated with the stress $\bar{\sigma}$ and of parameters chosen to characterize the damaged state of the material. The basic idea used by the micromechanical models (e.g. [29]) for dealing with damage consists in representing the microcracks as penny-shaped voids. By penny-shaped it is meant a spheroid, in which the length of its revolution axis is reduced to zero. Damage variables that characterize material microdefects are the crack density parameters d_i characterizing a family i of cracks having the same normal vector $\mathbf{e}_i$ associated with the driving forces Y_{di} defined in the ensuing. More precisely, these crack density parameters introduced by Budiansky and O'Connel [18] are defined as $d_i = N_i a_i^3$, where N_i is the volume density of the family i of microcracks and where a_i is the maximum axis of the degenerated spheroid representing the microcracks of type i. The damaged material is then viewed as a homogeneous matrix of cement-based material in which the microcracks are distributed. The idea of modelling these cracks as penny-shaped spheroids permits to account in an intuitive manner for the anisotropy caused by loads.

2.2. Micromechanical estimations of the damaged material behaviour

In the case of a strain formulation, the Helmhotz free energy practically corresponding to the energy stocked by elastic strains is written as:

$$\Phi = \frac{1}{2}\bar{\varepsilon} : \mathbb{C}^*(d_i) : \bar{\varepsilon}, \tag{1}$$

where the effective damaged stiffness tensor $\mathbb{C}^*$ depends on the homogenization scheme adopted. The Interaction Direct Derivative (IDD) estimate is presently chosen to compute this tensor, since it has been identified as rather suited for predicting the damaged mechanical properties of composites with aligned cracks [30,31]. The latter case is simple to treat analytically in the case where only one family of cracks with the same geometry and normal vectors assumed to be parallel to an axis denoted $\mathbf{e}_1$ is involved (the subscripts can thus be disregarded). For such materials, the following estimation of the effective stiffness tensor can be obtained by means of the IDD model [19], which coincides in this case with the scheme proposed by Ponte-Castaneda and Willis [32]:

$$\overset{*}{\mathbb{C}}_{IDD} = \left(\mathbb{S}_M + \mathbb{H}^{IDD}\right)^{-1}, \quad \text{with} \quad \mathbb{H}^{IDD} = \left(\mathbb{I} - \mathbb{H}^{dil} : \Omega_D^M\right)^{-1} : \mathbb{H}^{dil}, \quad (2)$$

where $\mathbb{H}^{dil}$ is called the dilute compliance increment tensor, $\mathbb{I}$ designates the fourth order identity tensor, $\mathbb{S}_M$ the compliance tensor of the undamaged material that behaves as a matrix entrapping the penny-shaped crack and $\Omega_D^M = C_M:(\mathbb{I} - \Sigma_D^M)$ denotes the eigenstiffness tensor of the double-inclusions surrounding the cracks, where $\mathbb{C}_M = \mathbb{S}_M^{-1}$ and $\mathbf{\Sigma}_D^M$ is their Eshelby tensor [33]. These double-inclusions practically characterize the spatial distribution of cracks [19,32] and are taken as spherical, since these defects are assumed to be isotropically dispersed. The tensor $\mathbb{H}^{dil}$ has got a simple expression, since the only non vanishing terms are [34]:

$$H_{1111}^{dil} = \frac{16\left(1-\nu^2\right)}{3E_M} d; \quad H_{1313}^{dil} = H_{1212}^{dil} = \frac{8\left(1-\nu^2\right)}{3(2-\nu)E_M} d, \quad (3)$$

where E_M and ν respectively designate the Young modulus and the Poisson ratio of the undamaged material and d is the damage variable characterizing the crack density in the direction $\mathbf{e}_1$. Closed-form expressions for the effective axial Young modulus E_1^* of the damaged material can then be derived from the previous equation [31]:

$$\frac{E_1^{IDD}}{E_M} = \left(1 - \frac{128d}{45}\right)\left[1 - \frac{128d}{45}\left(1 - \frac{45}{128\, d_C^{dil}}\right)\right]^{-1}, \text{with } d_C^{dil} = \frac{3}{16(1-\nu^2)}, \quad (4)$$

where d_C^{dil} corresponds to the critical crack density for which the dilute estimation of the Young modulus goes to zero.

In the ensuing, the damaged material considered to be in plane stress conditions is now supposed to be weakened by two families of perpendicular cracks numbered 1 and 2, which normal vectors are respectively oriented following two axes denoted as $\mathbf{e}_1$ and $\mathbf{e}_2$, respectively. This assumption allows for having a damage model that is tractable analytically. It furthermore permits to account in a certain manner for the anisotropy of a given material, as shown by the rosettes diagram proposed on Fig. 1 representing the relative decrease of the Young modulus along different orientations. Remark on this Figure that the cracks, which normal direction is for instance $\mathbf{e}_1$, influence the Young moduli in all the directions except the one perpendicular to $\mathbf{e}_1$. Thus, the system of perpendicular cracks, with crack density parameters such as $d_1 = d_2 = 0.1$, affects the Young modulus of the damaged material in all directions. According to this Figure, two families of perpendicular cracks seem to be sufficient for dealing with orthotropic cases. The present model should however not be applied for more complex anisotropic cases, for which additional families of cracks with different orientations would be required [35]. In the present study, the damage model developed will only be applied to simple cases of loadings. In the next Section, a reasoning about strain-based criteria [22,24] is carried out to establish an adequate evolution law for the damage parameters.

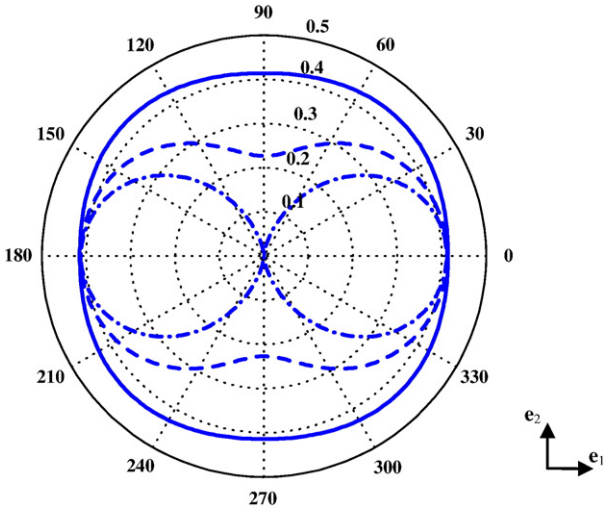

Fig. 1. Rosette representing the relative decrease of the effective Young modulus predicted by the IDD scheme for two families of cracks aligned with the $\mathbf{e}_1$ and $\mathbf{e}_2$ directions which crack densities are $d_1 = d$, $d_2 = 0$ with $d = 0.1$ (dash-dotted), $d_1 = d$, $d_2 = d/2$ (dashed) and $d_1 = d_2 = d$ (plain), respectively.

2.3. Establishment of a strain-based evolution law

The ensuing type of strain-based criterion inspired by the works of Mazars and Desmorat et al. [22,24] is proposed as a starting point:

$$f = \tilde{\varepsilon} - \kappa(\mathrm{tr}\mathbf{d}), \quad (5)$$

where $\tilde{\varepsilon}$ denotes an equivalent strain, the function $\kappa(\mathrm{tr}\mathbf{d})$ rules the evolution of the damage surface, tr denotes the trace of a tensor and $\mathbf{d}$ is a second-order micromechanical damage tensor that reads in the $(\mathbf{e}_1, \mathbf{e}_2, \mathbf{e}_3)$ orthonormal basis:

$$\mathbf{d} = \begin{pmatrix} d_1 & 0 & 0 \\ 0 & d_2 & 0 \\ 0 & 0 & 0 \end{pmatrix}, \quad (6)$$

since the normal vectors of the two families of perpendicular cracks retained in the micromechanical model are respectively oriented along $\mathbf{e}_1$ and $\mathbf{e}_2$. The equivalent strain proposed by De Vree et al. [36] and recalled below is capable of accounting for the differences of behaviour of cement-based materials in traction and in compression:

$$\tilde{\varepsilon}_{DV} = \frac{k-1}{2k(1-2\nu)} I_1^{(\varepsilon)} + \frac{1}{2k}\sqrt{\frac{(k-1)^2}{(1-2\nu)^2} I_1^{(\varepsilon)2} + \frac{12k}{(1+\nu)^2} J_2^{(\varepsilon)}}, \quad (7)$$

where the strain invariants are defined as:

$$I_1^{(\varepsilon)} = \mathrm{tr}\varepsilon \quad \text{and} \quad J_2^{(\varepsilon)} = \frac{1}{2}\mathrm{tr}\left(\varepsilon - \frac{1}{3}(\mathrm{tr}\varepsilon)1\right)^2, \quad (8)$$

where k denotes the ratio of the compressive strength over the tensile one. By analogy with Desmorat et al. [24], a simple expression is proposed for the dissipation potential:

$$\Psi^* = \mathbf{Y_d} : \langle \mathbf{R} \cdot \varepsilon_P \rangle_+^2, \quad (9)$$

where $\mathbf{Y_d} = -\partial\Phi/\partial\mathbf{d}$ is the driving force associated with the micromechanical damage tensor $\mathbf{d}$, $\mathbf{R}$ is a projection operator that projects the principal strain tensor on the $(\mathbf{e}_1, \mathbf{e}_2, \mathbf{e}_3)$ reference basis and $\boldsymbol{\varepsilon}_P$ is the tensor of the principal strains. This tensor admits the following representation:

$$\varepsilon_P = \varepsilon_I \mathbf{n}_I \otimes \mathbf{n}_I + \varepsilon_{II} \mathbf{n}_{II} \otimes \mathbf{n}_{II} + \varepsilon_{III} \mathbf{n}_{III} \otimes \mathbf{n}_{III}, \quad (10)$$

where ⊗ stands for the tensor product and $\mathbf{n}_i (i = \mathrm{I}, \mathrm{II}, \mathrm{III})$ are three orthonormal vectors defining the principal strain directions. The derivation of the dissipation potential yields the following non-associated evolution law:

$$\dot{\mathbf{d}} = \lambda \frac{\partial \Psi^*}{\partial \mathbf{Y_d}} = \lambda \langle \mathbf{R} \cdot \varepsilon_P \rangle_+^2. \tag{11}$$

An essential difference of the present approach with phenomenological models, such as the one of [24], is that the principal directions of the damage tensor are now fixed. The damage multiplier is then determined from the consistency condition and the damage evolution law takes the general form:

$$\dot{\mathbf{d}} = \frac{d\kappa^{-1}}{d\tilde{\varepsilon}_{DV}} \frac{\dot{\tilde{\varepsilon}}_{DV}}{\mathrm{tr}\langle \mathbf{R} \cdot \boldsymbol{\varepsilon}_P \rangle_+^2} \langle \mathbf{R}.\varepsilon_P \rangle_+^2. \tag{12}$$

Observe that the damage tensor rate is proportional to the square of the positive part of the principal strain tensor. The next stage consists in identifying a suitable function for $\kappa(\mathrm{tr}\mathbf{d})$. To perform such task, only one family of aligned cracks with normal vectors parallel to $\mathbf{e}_1$ is first considered for its simplicity. In the Mazars model [21,22], the elastic stiffness deterioration along the direction $\mathbf{e}_1$ is supposed to follow the evolution:

$$\frac{E_1^*}{E_M} = \exp\left(-B(\tilde{\varepsilon}_{Ma} - \varepsilon_0)\right), \tag{13}$$

where $\tilde{\varepsilon}_{Ma}$ is the Mazars equivalent strain [21,22] and where ε_0 designating the strain damage threshold and B are parameters that should be identified with different values in traction and in compression. It is furthermore recalled that the IDD estimations of the effective Young modulus E_1^* of the damaged material along the normal direction $\mathbf{e}_1$ to aligned cracks is expressed analytically as a function of the crack density parameter in Eq. (4). By combining this equation with Eq. (13), the following damage loading functions f_{IDD} can be established for the IDD damage model:

$$f_{IDD} = \frac{g(\tilde{\varepsilon}_{DV})}{g(\tilde{\varepsilon}_{DV}) + \frac{d_C^{IDD}}{d_C^{dil}}(1 - g(\tilde{\varepsilon}_{DV}))} - d_1, \text{ with} \tag{14}$$
$$g(\tilde{\varepsilon}_{DV}) = 1 - \exp(-B(\tilde{\varepsilon}_{DV} - \varepsilon_0)).$$

These damage loading functions can be extended to the case of two families by using the trace of the damage tensor $\mathbf{d}$:

$$f = \kappa^{-1}(\tilde{\varepsilon}_{DV}) - \mathrm{tr}\mathbf{d}. \tag{15}$$

It should be observed that only one criterion provides explicitly the evolutions of the two crack density parameters. The positivity of the intrinsic dissipation with the present strain-based criterion has been verified in Stora [31]. The non-linear stress–strain curve of the damaged material is then ruled by the rate form of Hooke's law reading:

$$\dot{\sigma} = \mathbb{C}^*(d_i) : \dot{\varepsilon} + \left(\frac{\partial \mathbb{C}^*}{\partial d_i} \dot{d}_i \right) : \varepsilon. \tag{16}$$

In the subsequent Section, the IDD damage model is implemented in the FE code CAST3M and simulations of three-point flexion tests of mortar samples subjected previously or simultaneously to accelerated leaching are performed and analysed.

3. Simulations of the residual mechanical behaviour of leached cement-based materials

The present Section is dedicated to the study of the influence of the chemical deterioration on the residual mechanical behaviour of cementitious materials. Residual resistance tests on concrete materials have been performed both in compression (e.g. [2,17,37]) and in traction or flexion (e.g. [4,8,9]). The simulations run with the ALLIANCES platform proposed below aims in particular at reproducing the flexion tests performed by Le Bellégo [4] on mortars that examine the effects of decalcification on their mechanical behaviour. The resolution of coupled chemical-transport problems such as leaching with the ALLIANCES platform is explained in the companion paper [16].

3.1. Simulations of mechanical residual resistance tests of a mortar beam

3.1.1. System considered

Different flexion tests exist in literature (e.g. [4,8,9]) for evaluating the mechanical residual resistance of cement-based materials. Le Bellégo [4] in particular conducted a large series of three-point bending tests of partially leached mortars and recorded the whole curve linking the displacement imposed and the reaction force. In the present simulations, the smallest beam tested by Le Bellégo [4] is used. Its total length and height are 320 mm and 80 mm, respectively. The lateral surfaces and the 60 mm long sections at the corners of the beam are insulated by an epoxy coating (see Fig. 2). Therefore only the central part of the lower face, which will be subsequently subjected to tensile stresses, is in contact with a 6 M NH_4NO_3 solution. The chemical attack of the beam by this aggressive solution lasts 114 days, which is roughly equivalent in terms of degradation depth to forty years of pure water leaching. Le Bellégo measured with phenolphthalein that the degradation depth reached 18.2 mm from the bottom of the beam.

After this attack, the deteriorated beam is further subjected to a three-point flexion test schematically represented in Fig. 2. The following mechanical boundary conditions are imposed:

$$u_y(x = 0, y = 0.08, t) = u_0; \quad u_x(x = 0, y, t) = 0; \quad u_y(x = 0.12, y = 0, t) = 0, \tag{17}$$

where the displacement u_0 is imposed on the center of the upper face of the beam, as may be seen in Fig. 2. The non-linear mechanical behaviour of the leached sample is then evaluated numerically via the FE code Cast3m using the micromechanically-based damage model detailed in Section 2. The beam is assumed to be in plane stress conditions. In the present system, eventual cracks inside the chemically degraded zone presently solicited in traction along the

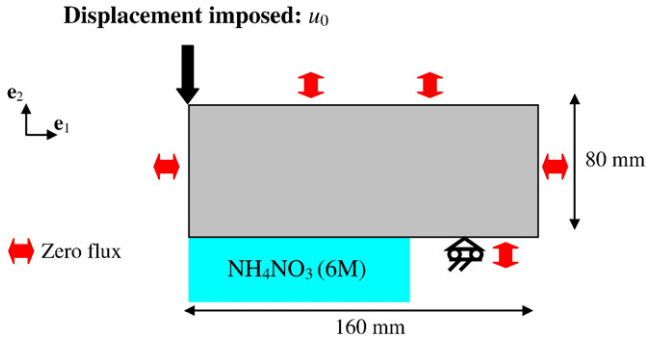

Fig. 2. Schematic of the system employed for the simulations of mechanical resistance tests and life-time experiments.

horizontal axis because of the flexural displacement imposed on the beam should mainly appear oriented parallel to the vertical axis.

A rather coarse 2D mesh comprising 1600 elements is employed for the chemo-transport and mechanical computations on the mortar beam, since the smallest element of the mesh should be bigger than the typical size of the RVE. It is recalled that this size is about 10–100 μm for cement pastes and about 1–10 mm for mortars. According to the work of Pensée and He [38] accounting for the effects of the size of the RVE, the latter should be significantly bigger than the typical sizes of the particulate phases. Lutz et al. [39] for example considered an average equivalent diameter of 700 μm for sand aggregates. The exact grading of the sand used can be found in Le Bellégo's thesis [4]. Consequently the average size of a mesh element should be at least superior to 2 mm in the case of mortars.

Concerning the representation of cracks, strong assumptions are made in the micromechanically-based damage model. They may grow in the bulk cement paste, through the interface between sand aggregates and paste and through the sand aggregates themselves. The micromechanical damage model consequently assumes that the cracks are embedded in an effective medium having the same properties as undamaged mortars, according to the fact that the cracks may grow anywhere. Another argument for representing the cracks inside the already homogenized undamaged mortars is that they may be extended and have a correlation length that is much longer than the particulate phase such as sand or clinker grains. In the case of concrete, cracks are also likely to grow inside and span over the coarse aggregates.

The chemical input data necessary for simulating this accelerated chemical degradation test are described in the companion paper [16]. In particular, the initial composition of the mortar beam is provided in Table 1 of the latter article. The clinker residuals and the sand aggregates are assumed for simplicity to be unaffected by NH_3NO_4 so that only the concentrations of hydrated cement phases evolve in the ensuing simulations. The multi-scale upscaling model presented in Stora et al. [16] provides the following estimations for the effective Young modulus and the diffusivity of sound mortar: $E^* = 38.2$ GPa and $D^* = 1.8\times10^{-12}$ m^2/s. The mechanical input data adopted for the damage model are: $\varepsilon_0 = 5\times10^{-5}$, $B = 7000$ and $k = 9.84$. The ratio k of the compressive strength over the tensile one is for example determined from the uniaxial compressive and tensile strengths provided by Le Bellégo [4], equal to 44.3 MPa and 4.5 MPa, respectively. The possible evolutions of the damage parameters with leaching are discussed in the next Section.

3.1.2. Evolutions of the damage threshold with leaching

Diverse methods have been proposed to model the evolution of damage with leaching [5,12,40]. Heukamp [6,17] performed interesting types of experiments testing in traction and compression both sound and uniformly leached samples of cement pastes. The results of his uniaxial tensile tests along the $\mathbf{e}_1$ axis on both sound and entirely leached HCP are depicted in Fig. 3. The maximum peak in the sound and uniformly leached pastes measured by Heukamp et al. [6] are reached at very different strain values equal to 8.6×10^{-5} and 2.7×10^{-4}, respectively. The stress–strain curves of these two samples obtained with the micromechanical models developed in Stora et al. [16] and in the present paper are also plotted in Fig. 3, illustrating the strong degradation of the mechanical properties of chemically deteriorated cement pastes. The relative decreases obtained for the Young moduli are quite close to the ones measured by Heukamp et al. [6]. Fig. 3 furthermore evidences the fact that the compressive or tensile strengths are strongly modified in the leached state. It raises an important question: how does the stress or strain damage threshold evolve during the decalcification process? Unfortunately, the decrease of strength for intermediate leached states is very difficult to measure because of the inhomogeneous degradation of the samples in the typical degradation tests. That's why the following assumption is made: damage occurs when the right line corresponding to the elastic part of the stress–strain curve of the decalcified material

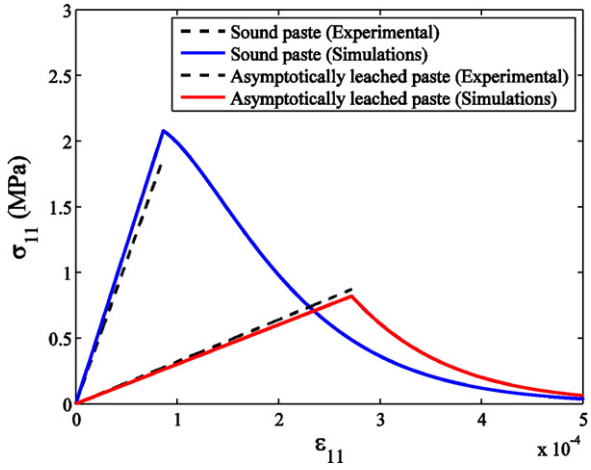

Fig. 3. Stress–strain curves of sound and uniformly leached cement pastes with w/c = 0.50 (Heukamp et al. 2005) submitted to a uniaxial traction following the $\mathbf{e}_1$ axis.

intersects the stress–strain curve of the damaged unleached material, as may be seen on Fig. 4. It practically means that an equivalency is supposed between the decay of the Young modulus due to damage and the one due to phase dissolution. The strain damage threshold $\varepsilon_0^{UL} = 2.37\times10^{-4}$ on Fig. 4 provided by this quite empirical method appears to be relatively close to the one $\varepsilon_0^{UL} = 2.72\times10^{-4}$ measured in Heukamp et al. [6] for the uniformly leached cement paste.

3.2. Results and comments

Before testing the residual mechanical resistance of the mortar beam, it is indispensable to first correctly reproduce the chemical deterioration of the material. The computation time for the numerical test of the accelerated leaching is about 3 h on a standard PC-Linux machine. The CH dissolution front reaches about 17 mm (Fig. 5) on mortar beams after 114 days of accelerated leaching. This depth is in quite good agreement with the one obtained experimentally by Le Bellégo despite the fact that the ion activities evaluated with the Davies modified method should be computed more accurately in the case of NH_4NO_3 attack. It appears on Fig. 6 that the calcium concentration in solution in contact with the 6 M NH_4NO_3 solution goes up to almost 2 mol/L near the portlandite dissolution front. This value is not far from the one considered by Tognazzi [1] and Heukamp

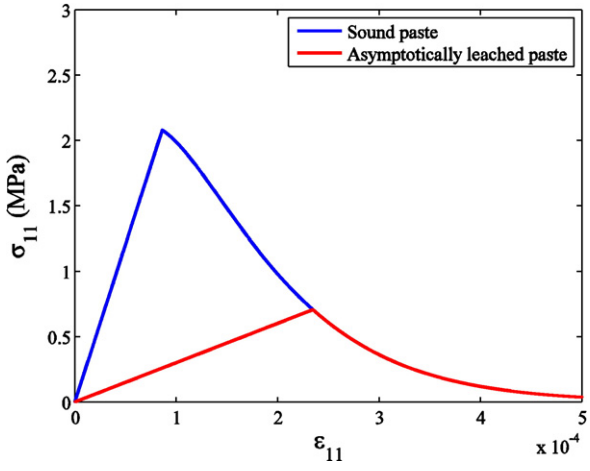

Fig. 4. Illustration of the method used to estimate the strain damage threshold of the leached paste from the stress–strain curve of the damaged unleached one.

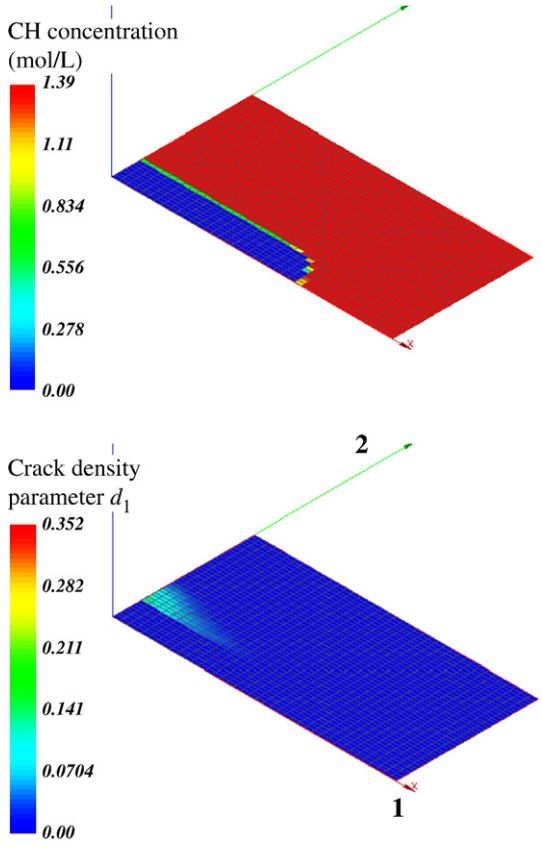

Fig. 5. Profile of the portlandite concentration (mol/L) in a mortar beam after a 114 days attack by a NH_4NO_3 solution (up); crack density parameter d_1 predicted by the IDD damage model in the leached beam submitted to a flexural displacement of 39.6 μm (down).

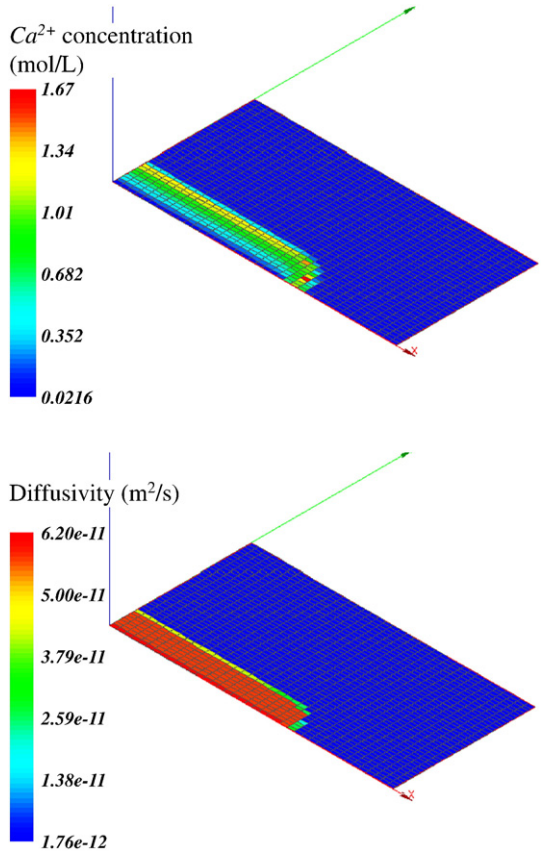

Fig. 6. Profiles of the diffusion coefficients (down) and of the liquid calcium concentration (mol/L) (up) in a mortar beam after a 114 days attack by a 6 M NH_4NO_3 solution.

[17], who assert that the CH dissolution front in the presence of a 6 M NH_4NO_3 solution occurs for a liquid calcium concentration inferior to 2.7 mol/L. In addition, the diffusivity in the leached zone of the beam (Fig. 6) augments by more than one order of magnitude compared with the sound part. The evolution of the mineral profile of mortar in the leached zone of the beam is plotted on Fig. 7 (left). The sequences of dissolution are similar to the ones observed in Stora et al. [16] and Moranville et al. [41] on a CEM I 42.5 paste after a pure water leaching. The degradation induced by a 6 M NH_4NO_3 solution being yet more severe than the one with pure water, the presence of a completely decalcified zone only composed with SiO_2(am) and diaspore may be seen on the left-hand side of Fig. 7 (left).

In order to correctly simulate the residual mechanical tests of Le Bellégo [4], it is necessary to first try to reproduce the results of her flexion tests performed on sound notched and unnotched mortar beams. According to Fig. 8, the maximum load supported by the sound beam is quite well predicted but the post-peak part of the simulated curve poorly fits with the experimental data. This could be explained by the fact that only a local version of the micromechanically-based model has been implemented in the platform. A non-local version of the model based on the work of Pijaudier-Cabot and Bazant [42] should however be incorporated in the future, since the simulations performed with 784, 1600 and 3600 elements, respectively, demonstrate a significant influence of the mesh (Fig. 8) in particular for the notched beam. In this case, the force–displacement curves appear to be strongly affected especially in terms of maximal load (and corresponding flexural displacement) and to a lesser extent of post-peak response.

In a first attempt, simulations of flexion tests on the leached mortar have been run using exactly the same values for the damage parameters as for the sound specimen. The results obtained appear on Fig. 8 (right) to be unsatisfactory thus confirming the fact that the damage threshold is modified by the leaching process. The empirical method described in Section 3.1.2 has therefore been employed to have the strain damage threshold ε_0 evolved. The pre-peak part of the numerical curve then agrees relatively well with the experimental curve on Fig. 8 (right) but the forces predicted by the simulations tend to be overestimated. There are diverse reasons to explain this difference. The first explanation could be that the Young modulus in the most leached zone, which is estimated to be equal to about 4.9 GPa by the multi-scale homogenization model, is overestimated, even though this value already seems to be quite low. For instance, Heukamp [17] measured that the effective Young modulus on a uniformly leached mortar is equal to 4.3 GPa. Another reason may be that the dissolution front propagation, that affects the material residual mechanical behaviour, is slightly underestimated in comparison with the one gained experimentally, as already asserted previously. Moreover, it could be also useful to adopt other values for the damage parameters A, B and k in order to better predict the residual resistance on leached mortars.

Fig. 5 also reveals the presence of a main damaged domain at the interface between the degraded and chemically sound parts of the beam. Conversely, the chemically leached zone is only slightly damaged, since the strain damage threshold in the decalcified region is assumed to increase rapidly with leaching (see Fig. 3). Further investigations concerning this evolution of the damage threshold with leaching would however be desirable to confirm this observation. Observe that the presently simulated experiment, designated as residual resistance test, does not account for the effects of damage on the chemical degradation process.

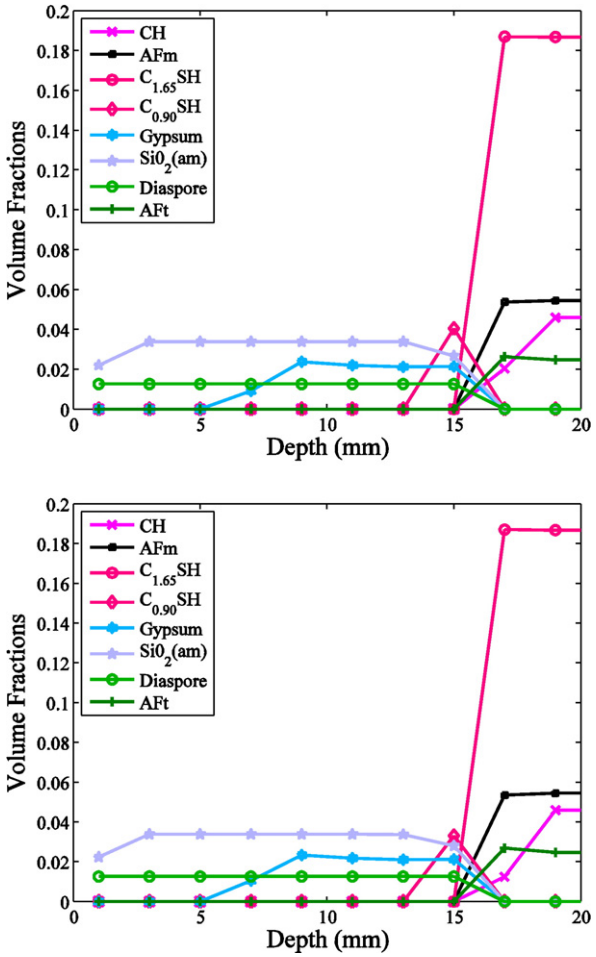

Fig. 7. Evolutions of the mineral compositions in terms of volume fractions inside a mortar beam after a 114 day attack by a NH_4NO_3 solution (left) and inside a mortar beam submitted simultaneously to an attack by a 6 M NH_4NO_3 solution on its lower face and to a flexural displacement during 112 days (right) along the vertical symmetry axis beam.

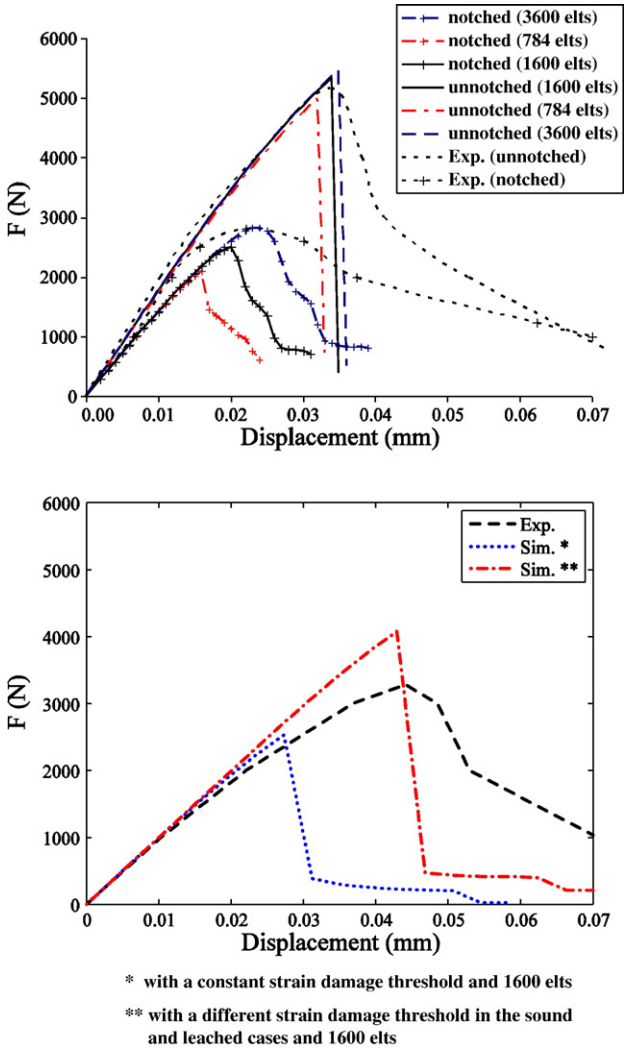

Fig. 8. Comparison of the simulation results with the experimental curve of the vertical forces plotted against the imposed flexural displacement recorded during a three-point flexion test on a sound mortar beam (left) and another one leached during 114 days by NH_4NO_3 (right).

4. Modelling the influence of cracks on leaching

The influence of decalcification on the damage evolution has been investigated in the preceding Section. In order to reproduce fully coupled chemo-mechanical deteriorations it is now necessary to find a way to model the retroactive effects of damage on leaching evidenced by experimentalists.

4.1. Evolutions of the diffusivity with damage

Chemical degradations are potentially influenced by the presence of microcracks because they may provide preferential pathways for fluid or ions to pass through. Many studies have reported that cracks can dramatically influence the transport properties of concrete, such as ionic diffusion (e.g. [1,43]) or permeability (e.g. [44]). Jacobsen et al. [43] investigated the effects of cracking on chloride transport in concrete and found that internal cracking increased the chloride penetration rate 2.5 to 8 times when compared with undamaged specimens. Tognazzi [1] carried out an experimental campaign to investigate the effects of damage induced by compressive or tensile loads on mortar effective diffusivity. First, displacement-controlled mechanical tests were performed on mortar specimens so as to generate different states of cracking. A visible impact of the damage created inside the material on its diffusivity increasing by 150–200% was noticed for samples having attained the post-peak regime of the mechanical test. This influence may be attributed to the coalescence of cracks. On the contrary, load induced damage does not appear to influence the diffusion properties substantially at the peak load due to the discontinuous and localized nature of the crack pattern. It is also noteworthy that Yang et al. [45] draw the same type of conclusions in their work on water absorption and electrical conductivity of concrete damaged by tensile loading and freeze and thaw cycling.

4.2. Evolutions of the diffusivity with damage

Let us assume a material weakened with aligned cracks that are all perpendicular to the $\mathbf{e}_1$ axis. In such occurrence, the formula for the material effective diffusivity tensor given by the IDD estimate that is very similar to the one in mechanics (Eq. (2)) takes the form:

$$\mathbf{D}^{\mathrm{IDD}} = \left[\mathbf{1} + \mathbf{D}_{\mathrm{M}}\cdot\mathbf{H}^{\mathrm{IDD}}\right]^{-1}\cdot\mathbf{D}_{\mathrm{M}},\ \text{with}\,\mathbf{H}^{\mathrm{IDD}} = \mathbf{H}^{\mathrm{dil}}\cdot\left[\mathbf{1}-\mathbf{H}^{\mathrm{dil}}\cdot\boldsymbol{\Theta}_{\mathrm{D}}^{\mathrm{M}}\right]^{-1},$$
$$\mathbf{H}^{\mathrm{dil}} = c_1\mathbf{H}_1\cdot\left[\mathbf{1} + \Theta_1^{\mathrm{M}}\cdot\mathbf{H}_1\right]^{-1}\text{and}\,\mathbf{H}_1 = \mathbf{D}_1^{-1} - \mathbf{D}_{\mathrm{M}}^{-1}, \tag{18}$$

where $\mathbf{D}_{\mathrm{M}}$ denotes the diffusivity tensor of the undamaged material, $\mathbf{D}_1$ the one of microcracks, $\mathbf{1}$ the second-order identity tensor, $\boldsymbol{\Theta}_1^{\mathrm{M}} = \mathbf{D}_M\cdot(\mathbf{1}-\mathbf{A}_1)$ the eigendiffusivity tensor of the microcracks

with normal vectors oriented along the $\mathbf{e}_1$ axis, c_1 their volume fractions and $\mathbf{\Theta}_D^M = \mathbf{D}_M \cdot (\mathbf{1} - \mathbf{A}_D)$ designates the eigendiffusivity tensor of the double-inclusion embedding these microcracks. The tensors $\mathbf{A}_1$ and $\mathbf{A}_D$ denote the Eshelby tensors [33] in diffusion of the microcracks and of the double-inclusion, respectively. Cracks being considered as isotropically distributed, the double-inclusion is spherical and $\mathbf{A}_D$ is simply equal to $(1/3)\mathbf{1}$ (e.g. [46]). The Eshelby tensor $\mathbf{A}_1$ of the aligned microcracks represented as oblate spheroids with aspect ratio r, which revolution axis is oriented along the $\mathbf{e}_1$ axis, is also analytically calculable (e.g. [46]) and can be expressed as:

$$\mathbf{A}_1 = \begin{bmatrix} 1-2Q & 0 & 0 \\ 0 & Q & 0 \\ 0 & 0 & Q \end{bmatrix}, \quad \text{with} \quad Q = \frac{1}{2}\left[1 + \frac{1}{r^2-1}\left[1 - \frac{r}{\sqrt{1-r^2}}\tan^{-1}\left(\frac{r}{\sqrt{1-r^2}}\right)\right]\right], \quad r \leq 1. \tag{19}$$

By combining the last two equations, the following IDD estimation is obtained for the diffusivity tensor of the anisotropic damaged body:

$$\mathbf{D}^{IDD} = \mathbf{D}_M \cdot \begin{bmatrix} 1 - \dfrac{3c_1\delta D}{3 + [3(1-2Q) + 2c_1]\delta D} & 0 & 0 \\ 0 & 1 - \dfrac{3c_1\delta D}{3 + [3Q + 2c_1]\delta D} & 0 \\ 0 & 0 & 1 - \dfrac{3c_1\delta D}{3 + [3Q + 2c_1]\delta D} \end{bmatrix}, \quad \text{with } \delta D = \frac{D_1 - D_M}{D_M}. \tag{20}$$

Small aspect ratios should be chosen for the oblate spheroids representing the microcracks. In order to find a reasonable value for this parameter, let us consider the simple traction test on mortar samples presented in Section 2 with a strain imposed attaining 3×10^{-4}. Considering that the diffusivities of cracks assumed to be saturated with water and of the mortar are equal to $D_1 = 2.2\times10^{-9}$ m^2/s and $D_M = 1.7\times10^{-12}$ m^2/s [47], the effect of damage on the diffusivity perpendicular to the $\mathbf{e}_1$ axis is then computed by means of Eq. (20) with two different values for the aspect ratio: $r = 10^{-3}$ and $r = 5\times10^{-3}$. The following values are then respectively obtained for the effective diffusivity of the damaged mortar along the $\mathbf{e}_2$ axis: $D_{22}^{IDD} = 2.1\times10^{-12}$ m^2/s and $D_{22}^{IDD} = 4.1\times10^{-12}$ m^2/s. The first value is nearly the same as the intact mortar diffusivity and is likely to have a negligible impact compared for instance with the diffusivities obtained in the leached zones of the mortar beam on Fig. 6. Conversely, the second computed value is two times bigger than the initial diffusion coefficient of the sound mortar and may thus have an influence on the leaching front propagation. The aspect ratio is consequently chosen equal to $r = 5\times10^{-3}$ as in Shao et al. [48] in the ensuing, even though further investigations would be necessary to better characterize this aspect ratio. To illustrate more precisely the effect of damage on diffusivity, the sound notched mortar beam used in Section 3 is considered to be subjected to a flexural displacement of 18 μm at the centre of its upper face. This displacement, which is close to the one corresponding to the maximum peak of the force–displacement curve on Fig. 8 (left), provokes the apparition of cracks in the beam. The mortar diffusivity along the $\mathbf{e}_2$ axis is then seen to increase slightly around the notch, where cracks have started to form (Fig. 9).

The individual effects of leaching on damage evolution and conversely of cracks on the decalcification have been investigated in the last two Sections. Hence, the next one is concerned with the simulations of life-time experiments, in which the decalcification process and damage evolution fully interact.

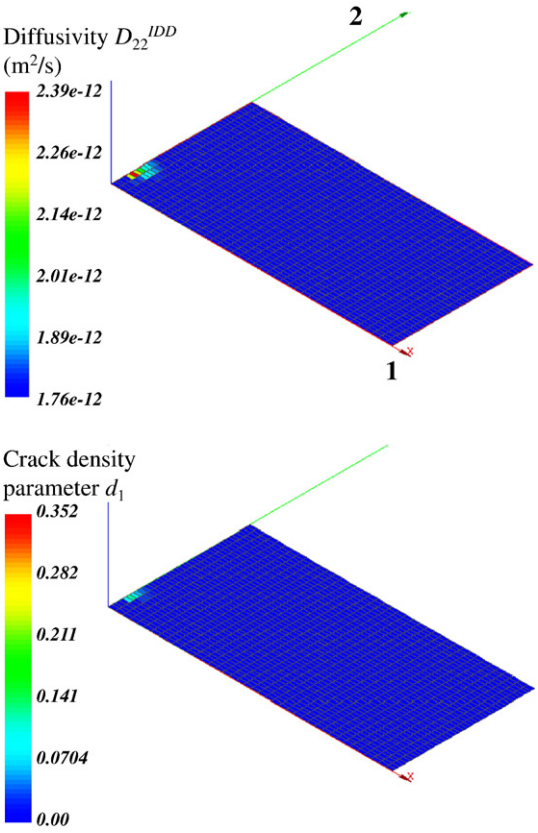

Fig. 9. Profiles of the diffusivity in the $\mathbf{e}_2$ direction (up) and of crack density parameter d_1 predicted by the IDD damage model (down) in an unleached mortar beam submitted to a flexural displacement of 18 μm.

5. Simulations of fully coupled chemo-mechanical tests of cement-based materials

Besides her residual resistance test presented in Section 3, Le Bellégo [4] has also carried out on a similar mortar beam a life-time experiment, in which the inferior part of the beam is simultaneously solicited in traction because of a flexural displacement imposed at the center of the upper face and put in contact with a 6 M NH_4NO_3 solution during 112 days (Fig. 2). This part of the beam is then both chemically degraded and subjected to tensile stresses, which are very likely to generate in this zone open cracks susceptible to enhance the leaching process. Crack propagation and chemical degradation are thus entirely coupled in this test. Its settings are similar to the ones of the residual resistance experiment described in Section 3 except that a flexural displacement $u_y(x = 0,\ y = 0.08) = 18$ μm is imposed on the centre of the upper face of the notched mortar beam during the 112 days of 6 M NH_4NO_3 leaching process. This displacement is chosen rather small to limit the creep effects. After this coupled chemo-mechanical attack of the beam, the residual mechanical behaviour is tested by incrementing stepwise the flexural displacement imposed.

Such coupled experimentations are difficult to simulate without making strong assumptions. Creep phenomena are not taken into consideration and the cracks are assumed to be instantaneously saturated. The first hypothesis is justified to a certain extent by the fact that the imposed flexural displacement is only 18 μm, which is smaller than the displacement of about 25 μm corresponding to the maximum peak of the notched beam response (Fig. 8). Despite these limitations, the simulation of the life-time test proposed gives some interesting results. According to Fig. 10, the influence of cracks on the diffusivity as modelled in Section 4.2 is much less important than the

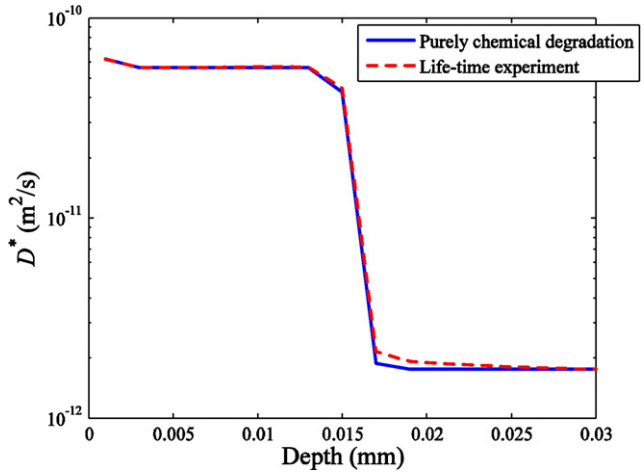

Fig. 10. Evolutions of the diffusivity inside a mortar beam after a 114 days attack by a NH_4NO_3 solution (dashed) and inside a mortar beam submitted simultaneously to an attack by a 6 M NH_4NO_3 solution on its lower face and to a flexural displacement during 112 days (plain) along the vertical symmetry axis beam.

effects of the dissolution due to leaching that may augment the mortar diffusivity by a few orders of magnitude. Consequently, the profiles of CH concentration are similar after 112 days of coupled chemo-mechanical deteriorations (Fig. 11) and after 114 days of accelerated leaching (Fig. 5 up). Fig. 7 (right) further shows that the cracks induced by the flexion imposed only enhance the dissolution process by a few days. Nonetheless, these cracks seem to have a stronger influence on the further development of cracks by comparing Figs. 5 (down) and 12. More precisely, two cracked zones, one in the decalcified region of the beam and the other one in the unleached part, are seen to form on Fig. 12 (up), whereas only one domain near the interface with the leached part of the beam gets damaged in Fig. 5 (down). As a consequence, the cracks propagate more in the life-time simulation (Fig. 12 down) than in the residual resistance one (Fig. 5 down) at a same level of flexural displacement. The present result provides a plausible explanation for the lower strength value noticed by Le Bellégo in this fully coupled experiment compared with the previous residual mechanical test. Nevertheless, this decay may also be caused at least partly by creep.

To summarize, the numerical results displayed on Figs. 10–12 tend to show that the life-time test is more detrimental than the residual resistance one mainly because it generates cracks both in the leached and sound zones of the beam that favour their further propagation. These cracks also enhance the leaching process but the acceleration obtained is not so significant probably due to the fact that their aperture is quite low in the test. Nonetheless, this simulation of life-time test has to be deemed with a lot of precautions for the subsequent reasons. First, modelling the influence of cracks on the material diffusive properties with homogenization techniques is not a trivial matter because of the difficulty of accounting for the connectivity between cracks that is not reproduced by the IDD scheme. The reader should refer to some authors [49] who have worked more specifically on this aspect. The results presented also depend on the mesh adopted, since only a local version of the micromechanically-based damage model has been implemented in the platform. Creep phenomena are furthermore not taken into consideration for simplicity. A non-local formulation of the damage model and the incorporation of creep effects are key points to make more consistent simulations in the future.

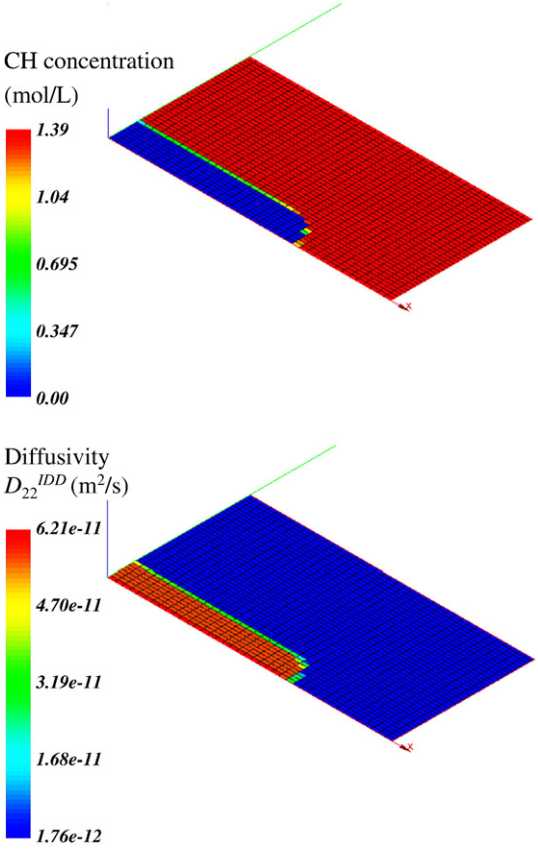

Fig. 11. Profiles of diffusivity in the e_2 direction (down) and of the portlandite concentration (up) in a mortar beam submitted simultaneously to an attack by a 6 M NH_4NO_3 solution on its lower face and to a flexural displacement of 18 μm during 112 days.

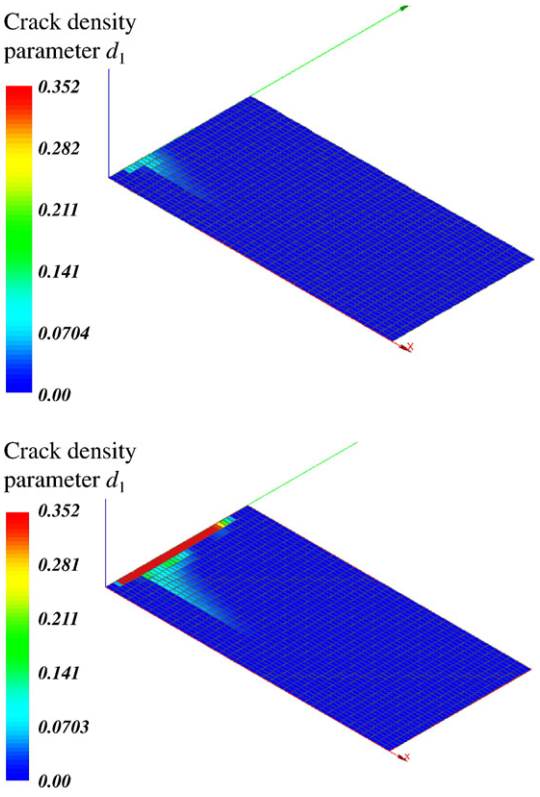

Fig. 12. Crack density parameter d_1 predicted by the IDD damage model in a beam subjected simultaneously to an attack by a 6 M NH_4NO_3 solution on its lower face and to a flexural displacement of 18 μm during 112 days subsequently submitted to a flexural displacement of 29 (up) and 39.6 μm (down).

6. Conclusions

The present paper and its companion one [16] have been devoted to the development of a general tool incorporated in the ALLIANCES numerical platform that allows for estimating the long-term evolutions of the mineral composition of leached cementitious materials and of their mechanical and diffusive properties. For this purpose, a multi-scale homogenization approach [16] and a micromechanical damage model have been proposed and implemented into the ALLIANCES platform to predict the evolutions of the diffusivity and mechanical behaviour of cement-based materials. The use of micromechanical concepts turns out to be a promising method to compute the retroactive effects of cracks on the chemical degradation.

With the help of the numerical device developed, simulations of the chemo-mechanical behaviour of decalcified cement-based materials have been carried out. Both residual resistance and life-time experiments illustrating the couplings between damage and leaching have been simulated. The numerical results give some interesting interpretations summarized below that are particularly useful for assessing the durability of cement-based materials. First, the simulated behaviour of sound and leached mortar beams in flexion has underlined the necessity to have the damage threshold presently expressed in deformations evolved with decalcification. An empirical method that assimilates the decrease of the Young modulus due to leaching to the one caused by damage is then employed to predict more accurately the maximum load that the deteriorated material can sustain. According to this method, the formation of cracks is then influenced by decalcification, the leached zones being less microcracked than the chemically sound ones. In addition, two effects of crack formation on the material long-term behaviour have been investigated through the simulation of life-time tests: (i) the influence of the generated cracks on the material residual mechanical behaviour; and (ii) their impact on the diffusive properties and on the leaching process. The numerical results tend to show that the first effect is more pronounced than the second one.

These observations require however to be further discussed and validated given some of the strong approximations made in this study. The prediction of the evolution of damage initiation with leaching needs to be improved for instance through the use of non-linear homogenization methods (e.g. [50,51]). Some further refinement may also be necessary for the modelling of damage inside the material in order to include phenomena such as frictional effects, plasticity or creep. While the latter phenomenon may be of great importance in the context of long-term waste disposal, plasticity would be useful to describe the residual strains appearing when the material is subjected to tension-compression loading paths. The integration of a non-local formulation is also central to get better estimations of the post-peak behaviour of the damaged material. Moreover, the impact of damage on diffusive properties would deserve additional experimental as well as modelling investigations and validations.

The proposed results are of direct interest in the context of nuclear waste disposal but the applications of the numerical tool developed can be noticeably broadened. It could for instance be applied to diverse types of chemical attacks, such as sulfate attacks generating internal pressures and possibly microcracks. The present work is more generally justified by the increasing necessity of adopting coupled multi-physical approaches for the assessment of the life-time of existing structures. In the perspective of concrete durability, more and more investigations are dedicated to coupled multi-physical problems, like the present one or thermo-hydro-mechanical ones (e.g. [52]). This study combined with other approaches (e.g. [25]) could lead at term to the development of powerful prediction tools for the durability of concrete facilities. It constitutes a huge task because of the necessity of solving thorny issues, such as unsaturated conditions. These tools would then find very wide industrial applications in the nuclear as well as in the civil engineering context.

Acknowledgments

Financial support from DEN/DSNI/Réacteur and DSOE STOEN is gratefully acknowledged.

References

[1] C. Tognazzi, Couplage fissuration-dégradation chimique dans les matériaux cimentaires: caractérisation et modélisation, PhD thesis, INSA Toulouse, France, 1998 (in French).
[2] C. Carde, Caractérisation et modélisation de l'altération des propriétés mécaniques due à la lixiviation des matériaux cimentaires, PhD thesis, INSA Toulouse, France, 1996 (in French).
[3] C. Gallé, H. Peycelon, P. Le Bescop, Effect of an accelerated chemical degradation on water permeability and pore structure of cement-based materials, Adv. Cem. Res. 16 (3) (2004) 105–114.
[4] C. Le Bellégo, Couplages chimie-mecanique dans les structures en béton attaquées par l'eau: Etude expérimentale et analyse numérique, PhD thesis, ENS Cachan, France, 2001 (in French).
[5] C. Le Bellégo, G. Pijaudier-Cabot, B. Gérard, J.F. Dubé, L. Molez, Coupled mechanical and chemical damage in calcium leached cementitious structures, J. Eng. Mech. 129 (3) (2003) 333–341.
[6] F.H. Heukamp, F.-J. Ulm, J.T. Germaine, Does calcium leaching increase ductility of cementitious materials? Evidence from direct tensile tests, J. Mater. Civ. Eng. 307 (2005).
[7] V.H. Nguyen, Couplage dégradation chimique—comportement en compression du béton, PhD thesis, ENPC, France, 2005 (in French).
[8] U. Schneider, S.W. Chen, Deterioration of high-performance concrete subjected to attack by the combination of ammonium nitrate solution and flexure stress, Cem. Concr. Res. 35 (9) (2005) 1705–1713.
[9] U. Schneider, S.W. Chen, The chemomechanical effect and the mechanochemical effect on high-performance concrete subjected to stress corrosion, Cem. Concr. Res. 28 (4) (1998) 509–522.
[10] P. Montarnal, A. Bengaouer, C. Chavant, L. Loth, ALLIANCES: Simulation Platform for Nuclear Waste Disposal, Proceedings of the CMWR'06, Copenhagen, Denmark, 2006.
[11] P. Montarnal, C. Mügler, J. Colin, M. Descotes, A. Dimier, E. Jacquot, Presentation and use of a reactive transport code in porous media, to appear in Phys. Chem. Earth. (2007).
[12] B. Gérard, Contribution des couplages mécanique-chimie-transfert dans la tenue á long terme des ouvrages de stockage de déchets radioactifs, PhD thesis, ENS Cachan, France, 1996 (in French).
[13] D. Kuhl, F. Bangert, G. Meschke, Coupled chemo-mechanical deterioration of cementitious materials Part II: Numerical methods and simulations, Int. J. Solids Struct. 41 (1) (2004) 41–67.
[14] D. Kuhl, F. Bangert, G. Meschke, Coupled chemo-mechanical deterioration of cementitious materials. Part I: Modeling, Int. J. Solids Struct. 41 (1) (2004) 15–40.
[15] B. Bary, Simplified coupled chemo-mechanical modeling of cement pastes behavior subjected to combined leaching and external sulfate attack, accepted for publication in Int. J. Num. Ana. Meth. Geomech. 32 (14) (2008) 1791–1816.
[16] E. Stora, B. Bary, Q.-C. He, E. Deville, P. Montarnal, Modelling and simulations of the chemo-mechanical behaviour of leached cement-based materials: leaching process and induced loss of stiffness, Cem. Concr. Res. 39 (9) (2009) 763–772.
[17] F.H. Heukamp, Chemomechanics of calcium leaching of cement-based materials at different scales: the role of CH dissolution and CSH degradation on strength and durability performance of maerials and structure, PhD thesis, Cambridge, 2002.
[18] B. Budiansky, R.J. O'Connell, Elastic moduli of a cracked solid, Int. J. Solids Struct. 12 (1976) 81–97.
[19] Q.S. Zheng, D.X. Du, An explicit and universally applicable estimate for the effective properties of multiphase composites which accounts for inclusion distribution, J. Mech. Phys. Solids 49 (11) (2001) 2765–2788.
[20] D. Krajcinovic, Damage Mechanics, North-Holland, Amsterdam, 1996.
[21] J. Mazars, Description of micro- and macroscale damage of concrete structures, Eng. Frac. Mech. 25 (5–6) (1985) 729–737.
[22] J. Mazars, Application de la mécanique de l'endommagement au comportement non linéaire et à la rupture du béton de structure, PhD thesis, Université de Paris VI, 1984 (in French).
[23] E. Papa, A damage model for concrete subjected to fatigue loading, Eur. J. Mech. A/Solids 12 (1993) 429–440.
[24] R. Desmorat, F. Gatuingt, F. Ragueneau, Nonlocal anisotropic damage model and related computational aspects for quasi-brittle materials, Eng. Frac. Mech. 74 (10) (2007) 1539–1560.
[25] B. Bary, S. Durand, G. Ranc, O. Carpentier, A coupled thermo-hydro-mechanical model for concrete subjected to moderate temperatures, Int. J. Heat Mass Transfer 51 (11–12) (2008) 2847–2862.
[26] Q. Zhu, D. Kondo, J. Shao, V. Pensee, Micromechanical modelling of anisotropic damage in brittle rocks and application, Int. J. Rock Mech. Mining Sci., 45 (4) (2008) 467–477.
[27] Q.-C. He, A. Curnier, A more fundamental approach to damaged elastic stress–strain relations, Int. J. Solids Struct. 32 (10) (1995) 1433–1457.
[28] Q. Nguyen, Stability and Nonlinear Solid Mechanics, Wiley, Chichester, 2000.
[29] M. Kachanov, Effective elastic properties of cracked solids: critical review of some basic concepts, Appl. Mech. Rev. 45 (1992) 304–335.
[30] X.-Q. Feng, J.-Y. Li, L. Ma, S.-W. Yu, Analysis on interaction of numerous microcracks, Comp. Mater. Sci. 28 (3–4) (2003) 454–462.

[31] E. Stora, Multi-scale modelling and simulations of the chemo-mechanical behavior of degraded materials, PhD thesis, University of Paris-Est Marne-la-Vallée, 2007.
[32] P. Ponte Castaneda, J.R. Willis, The effect of spatial distribution on the effective behavior of composite materials and cracked media, J. Mech. Phys. Solids 43 (12) (1995) 1919–1951.
[33] J.D. Eshelby, The determination of the elastic field of an ellipsoidal inclusion and related problems, Proc. Roy. Soc. London Ser. A-Math. Phys. Sci. 241 (1226) (1957) 376–396.
[34] T. Mura, Micromechanics of Defects in Solids, Martinus Nijhoff, The Hague, 1987.
[35] V. Pensée, D. Kondo, Micromechanics of anisotropic brittle damage: comparative analysis between a stress based and a strain based formulation, Mech. Mater. 35 (8) (2003) 747–761.
[36] J. De Vree, W. Brekelmans, M. Van Gils, Comparison of nonlocal approaches in continuum damage mechanics, Comp. Struct. 55 (1995) 581–588.
[37] Agostini, Z. Lafhaj, F. Skoczylas, H. Loodsveldt, et al., Experimental study of accelerated leaching on hollow cylinders of mortar, Cem. Concr. Res. 37 (2007) 71–78.
[38] V. Pensée, Q.-C. He, Generalized self-consistent estimation of the apparent isotropic elastic moduli and minimum representative volume element size of heterogeneous media, Int. J. Solids Struct. 44 (2007) 2225–2243.
[39] M.P. Lutz, P.J.M. Monteiro, R.W. Zimmerman, Inhomogeneous interfacial transition zone model for the bulk modulus of mortar, Cem. Concr. Res. 27 (7) (1997) 1113–1122.
[40] F.-J. Ulm, O. Coussy, Strength growth as chemo-plastic hardening in early age concrete, J. Eng. Mech. 122 (12) (1996) 1123–1131.
[41] M. Moranville, S. Kamali, E. Guillon, Physicochemical equilibria of cement-based materials in aggressive environments-experiment and modeling, Cem. Concr. Res. 34 (9) (2004) 1569–1578.
[42] G. Pijaudier-Cabot, Z.P. Bazant, Non local damage theory, J. Eng. Mech. 113 (1987) 1512–1533.
[43] S. Jacobsen, J. Marchand, L. Boisvert, Effect of cracking and healing on chloride transport in OPC concrete, Cem. Concr. Res. 26 (6) (1996) 869–881.
[44] K. Wang, D.C. Jansen, S.P. Shah, Permeability study of cracked concrete, Cem. Concr. Res. 27 (3) (1997) 381–393.
[45] Z. Yang, W.J. Weiss, J. Olek, Water transport in concrete damaged by tensile loading and freeze–thaw cycling, J. Mater. Civ. Eng. 18 (3) (2006) 424–434.
[46] S. Torquato, Random Heterogeneous Media: Microstructure and Macroscopic Properties, Springer-Verlag, New York, 2001.
[47] B. Bourdette, Durabilité du mortier, prise en compte des auréoles de transition dans la caractérisation et la modélisation des processus physiques et chimiques d'altération, PhD thesis, INSA Toulouse, France, 1994 (in French).
[48] J.F. Shao, H. Zhou, K.T. Chau, Coupling between anisotropic damage and permeability variation in brittle rocks, Int. J. Num. Ana. Meth. Geomech. 29 (12) (2005) 1231–1247.
[49] L. Dormieux, D. Kondo, Micromechanical approach to the coupling between permeability and damage [Approche micromécanique du couplage perméabilité-endommagement], C. R. Méca. 332 (2) (2004) 135–140.
[50] P. Suquet, Effective behavior of non linear composites, continuum micromechanics, CISM Courses and Lectures, 1997.
[51] J. Sanahuja, L. Dormieux, Résistance d'un milieu poreux à phase solide hétérogène, C. R. Méca 333 (11) (2005) 818–823.
[52] D. Gawin, C.E. Majorana, B.A. Schrefler, Numerical analysis of hygro-thermal behaviour and damage of concrete at high temperature, Mech. Cohesive-Frictional Mater. 4 (1) (1999) 37–74.